

## Phase control in the vibrational qubit

Meiyu Zhao and Dmitri Babikov<sup>a)</sup>

Chemistry Department, Wehr Chemistry Building, Marquette University, Milwaukee, Wisconsin 53201-1881

(Received 10 April 2006; accepted 12 June 2006; published online 14 July 2006)

In order to use molecular vibrations for quantum information processing one should be able to shape infrared laser pulses so that they can play the role of accurate quantum gates and drive the required vibrational transitions. In this paper we studied theoretically how the relative phase of the optimized transitions affects accuracy of the quantum gates in such a system. Optimal control theory and numerical propagation of laser-driven vibrational wave packets were employed. The dependencies observed for one-qubit gates NOT,  $\pi$ -rotation, and Hadamard transform are qualitatively similar to each other. The results of the numerical tests agree well with the analytical predictions.

© 2006 American Institute of Physics. [DOI: 10.1063/1.2220039]

### I. INTRODUCTION

In recent years the possibility of using vibrational eigenstates of molecules for quantum computation (QC) has been explored in a number of theoretical papers.<sup>1–11</sup> In such a vibrational quantum computer the quantum information bits (qubits) are encoded in the normal vibration modes of molecules. The quantum gates are applied using the femtosecond infrared laser pulses shaped adaptively to induce the desired state-to-state transitions.

In order to theoretically design a shape for the pulse which can serve as a quantum gate the monotonically convergent numerical algorithm derived from the optimal control theory<sup>12</sup> (OCT algorithm) is usually employed. In its traditional implementation the OCT algorithm is used to optimize the pulse shape  $\varepsilon(t)$  for a transfer of the entire population from the given initial vibrational state  $\phi_i$  to a chosen final state  $\phi_f$  within the time interval  $T$ . This is achieved by maximizing a relatively simple objective functional.<sup>12–14</sup> For quantum computation, however, the laser pulse should carry out a unitary transformation of the vibrational qubit states. For example, for the gate NOT we have to find a pulse which induces not just one but two transitions between the qubit states simultaneously:

$$\text{NOT}|0\rangle \rightarrow |1\rangle, \quad (1)$$

$$\text{NOT}|1\rangle \rightarrow |0\rangle. \quad (2)$$

This means that if the system was initially in the vibrational state  $|0\rangle$  it should be driven into state  $|1\rangle$ , but if it was initially in state  $|1\rangle$  it should be driven into state  $|0\rangle$ . One universal gate pulse should be able to perform each of these two transformations; which one is actually performed depends only on the initial state of the qubit. Therefore, it is required to optimize the population transfer in both transitions of interest simultaneously. Such a problem can be addressed by maximizing the functional where the sum over the two transitions of interest is introduced:<sup>2,5–10</sup>

$$K_{fi} \equiv - \int_0^T \alpha |\varepsilon(t)|^2 dt + \sum_{k=1,2} |\langle \psi_i^k(T) | \phi_f^k \rangle|^2 - \sum_{k=1,2} 2 \operatorname{Re} \left\{ \langle \psi_i^k(T) | \phi_f^k \rangle \int_0^T \langle \psi_f^k(t) | \left[ \frac{i}{\hbar} [H_0 - \mu \varepsilon(t)] + \frac{\partial}{\partial t} \right] \psi_i^k(t) dt \right\}. \quad (3)$$

Here index  $k=\{1,2\}$  labels two transitions, so that for the gate NOT, we set  $\phi_i^{(1)}=|0\rangle$ ,  $\phi_f^{(1)}=|1\rangle$  and  $\phi_i^{(2)}=|1\rangle$ ,  $\phi_f^{(2)}=|0\rangle$ . The  $\psi_i^k(t)$  are laser-driven time-dependent wave functions for each case, and  $\varepsilon(t)$  is the universal gate field. Each term  $|\langle \psi_i^k(T) | \phi_f^k \rangle|^2$  represents an overlap of the final wave function with the target state and these are maximized. The first term in (3) is required to minimize energy of the pulse and also to constrain its smooth switching on and off. The last term ensures that evolution of the wave functions  $\psi^k(t)$  satisfies the time-dependent Schrödinger equation; there  $H_0(r) = -(1/2m)\Delta_r + V(r)$  is the time-independent molecular Hamiltonian and  $\mu(r)$  is the molecular dipole moment function. Maximization of the functional (3) leads to a set of two time-dependent Schrödinger equations to be propagated forward and backward in time using  $\phi_i^k$  and  $\phi_f^k$ , respectively, as boundary conditions. The optimal field  $\varepsilon(t)$  is then determined iteratively.<sup>12</sup>

It was noted only recently<sup>7</sup> that although the two transition probabilities  $|\langle \psi_i^{(1)}(T) | \phi_f^{(1)} \rangle|^2$  and  $|\langle \psi_i^{(2)}(T) | \phi_f^{(2)} \rangle|^2$  are indeed maximized simultaneously in the functional (3), the final phases  $\varphi_1$  and  $\varphi_2$  of the two wave functions  $\psi_i^{(1)}(T)$  and  $\psi_i^{(2)}(T)$  remain totally independent and the phase difference is arbitrary. This means that instead of (1) and (2) the following two transitions are actually optimized:

$$|0\rangle \rightarrow |1\rangle e^{i\varphi_1}, \quad (4)$$

$$|1\rangle \rightarrow |0\rangle e^{i\varphi_2}, \quad \varphi_2 \neq \varphi_1. \quad (5)$$

Since the total phase of the wave function is irrelevant one can erroneously conclude that  $\varphi_2 \neq \varphi_1$  causes no problem whatsoever, but analysis presented in this paper shows that

<sup>a)</sup> Author to whom correspondence should be addressed. Electronic mail: dmitri.babikov@mu.edu

this is so only in two cases: when the initial state of the qubit is either  $|0\rangle$  or  $|1\rangle$ . In general transitions (4) and (5) do not represent the correct NOT transform of the qubit. The problem becomes evident when the pulse optimized for transitions (4) and (5) is applied to the qubit in a superposition state, for example,  $\frac{1}{\sqrt{2}}(|0\rangle+|1\rangle)$ . To overcome this drawback it was proposed<sup>7</sup> to include one more transition,

$$\frac{1}{\sqrt{2}}(|0\rangle+|1\rangle) \rightarrow \frac{1}{\sqrt{2}}(|1\rangle+|0\rangle)e^{i\varphi_3}, \quad (6)$$

for optimization simultaneously with transitions (4) and (5). Note that the purpose of this is not just to take care of the superposition state  $\frac{1}{\sqrt{2}}(|0\rangle+|1\rangle)$  as well, but rather to constrain the common phase in transitions (4) and (5). Indeed, when transitions (4)–(6) are optimized simultaneously and are driven by the same single laser pulse, their phases are guaranteed to be equal:  $\varphi_3=\varphi_2=\varphi_1$ . The value of this common phase can be arbitrary.

In this paper we explore this problem from a different perspective. In practice, the gate pulse can be obtained by optimizing only a small number of transitions (two or three as described above, for example). But in general, the qubit state can be any coherent superposition of states  $|0\rangle$  and  $|1\rangle$ :

$$\sqrt{\alpha}|0\rangle+\sqrt{1-\alpha}e^{i\theta}|1\rangle, \quad (7)$$

where  $\sqrt{\alpha}$  and  $\sqrt{1-\alpha}$  are the amplitudes ( $0\leq\alpha\leq 1$ ) and  $\theta$  is the phase difference ( $0\leq\theta\leq\pi$ ). Since  $\alpha$  and  $\theta$  change continuously there is an infinite number of initial qubit states and the truly universal quantum gate should be able to perform accurate transformation of the qubit for any values of  $\alpha$  and  $\theta$ . Therefore, it is instructive to obtain the gate pulse by optimizing only a few selected transitions and then study how this pulse performs when the values of  $\alpha$  and  $\theta$  are widely varied.

As a model of one-qubit system we used the diatomic molecule OH. The ground vibrational state ( $v=0$ ) of OH was used to represent  $|0\rangle$  state of a qubit while the first excited vibrational state ( $v=1$ ) was used to represent the qubit state  $|1\rangle$ . As usual, we restrict our considerations to the rotation frame (interaction picture) which allows to cancel the precession of the qubit state vector around the axis of the Bloch sphere caused by the energy difference of the  $v=0$  and  $v=1$  states. The QC treatment of OH diatomic was described in detail in our previous work<sup>6</sup> and also in a recent reference.<sup>11</sup> This molecule has also been considered as a benchmark system in several earlier coherent control studies.<sup>12,13,15</sup> In Sec. II of the paper we first study the gate NOT; this is the simplest case because the relative phase of qubit eigenstates is not affected by this gate. Then we consider the  $\pi$ -rotation gate and the Hadamard transform. Conclusions are outlined in the Sec. III.

## II. PHASE CONTROL

### A. Gate NOT

Transformation of an arbitrary initial qubit state (7) by the gate NOT is represented by

$$\text{NOT}(\sqrt{\alpha}|0\rangle+\sqrt{1-\alpha}e^{i\theta}|1\rangle) \rightarrow \sqrt{\alpha}|1\rangle+\sqrt{1-\alpha}e^{i\theta}|0\rangle. \quad (8)$$

The resultant qubit state in (8) should be considered as a target. Let us suppose that the pulse shape has been obtained by optimizing the two transitions (4) and (5). If such a pulse is applied to an arbitrary initial qubit state (7), the qubit will be transformed as follows:

$$\begin{aligned} \sqrt{\alpha}|0\rangle+\sqrt{1-\alpha}e^{i\theta}|1\rangle &\rightarrow \sqrt{\alpha}e^{i\varphi_1}|1\rangle+\sqrt{1-\alpha}e^{i\theta}e^{i\varphi_2}|0\rangle \\ &=(\sqrt{1-\alpha}e^{i\theta}|0\rangle+\sqrt{\alpha}e^{i(\varphi_1-\varphi_2)}|1\rangle)e^{i\varphi_2}. \end{aligned} \quad (9)$$

An overlap between the result (9) and the target (8) can be used to assess accuracy of the pulse transformation:

$$P=|\langle\psi_f(T)|\phi_f\rangle|^2=|\alpha+(1-\alpha)e^{-i(\varphi_2-\varphi_1)}|^2. \quad (10)$$

The readers can see that the transfer probability here depends not only on the initial qubit state (through  $\alpha$  only) but also on the phase difference  $\Delta\varphi=\varphi_2-\varphi_1$  of the optimized transitions (4) and (5).

As an alternative to transitions (4) and (5), the pulse shape for the gate NOT can be obtained by optimizing the two transitions which involve two superposition states:

$$\frac{1}{\sqrt{2}}(|0\rangle+|1\rangle) \rightarrow \frac{1}{\sqrt{2}}(|1\rangle+|0\rangle)e^{i\varphi_3}, \quad (11)$$

$$\frac{1}{\sqrt{2}}(|0\rangle-|1\rangle) \rightarrow \frac{1}{\sqrt{2}}(|1\rangle-|0\rangle)e^{i\varphi_4}, \quad \varphi_4\neq\varphi_3. \quad (12)$$

When such a pulse is applied to an arbitrary initial qubit state (7) the result is

$$\begin{aligned} \sqrt{\alpha}|0\rangle+\sqrt{1-\alpha}e^{i\theta}|1\rangle &\rightarrow \left[ \left( \frac{\sqrt{\alpha}1-e^{i(\varphi_4-\varphi_3)}}{2} \right. \right. \\ &\quad \left. \left. + \frac{\sqrt{1-\alpha}e^{i\theta}1+e^{i(\varphi_4-\varphi_3)}}{2} \right) |0\rangle \right. \\ &\quad \left. + \left( \frac{\sqrt{\alpha}1+e^{i(\varphi_4-\varphi_3)}}{2} \right. \right. \\ &\quad \left. \left. + \frac{\sqrt{1-\alpha}e^{i\theta}1-e^{i(\varphi_4-\varphi_3)}}{2} \right) |1\rangle \right] e^{i\varphi_3}. \end{aligned} \quad (13)$$

This formula was derived by adding and subtracting Eqs. (11) and (12) in order to obtain transformation of the two qubit eigenstates  $|0\rangle$  and  $|1\rangle$ . In this case, for the transfer probability we obtain

$$\begin{aligned} P=|\langle\psi_f(T)|\phi_f\rangle|^2 &= \left| \frac{1+e^{-i(\varphi_4-\varphi_3)}}{2} + \frac{\sqrt{\alpha(1-\alpha)}}{2}(e^{i\theta}+e^{-i\theta}) \right. \\ &\quad \left. \times (1-e^{-i(\varphi_4-\varphi_3)}) \right|^2. \end{aligned} \quad (14)$$

Again, the pulse quality depends on the phase difference  $\Delta\varphi=\varphi_4-\varphi_3$  between the two optimized transitions (11) and (12). The effect of the initial qubit state is now through both  $\alpha$  and  $\theta$ . Analysis of either (10) or (14) shows that the unit transfer probability  $P=1$  is always achieved when the initial qubit state is the one used for optimization of the laser pulse, even if the  $\Delta\varphi\neq 0$ . However, when  $\alpha$  and  $\theta$  are changed the

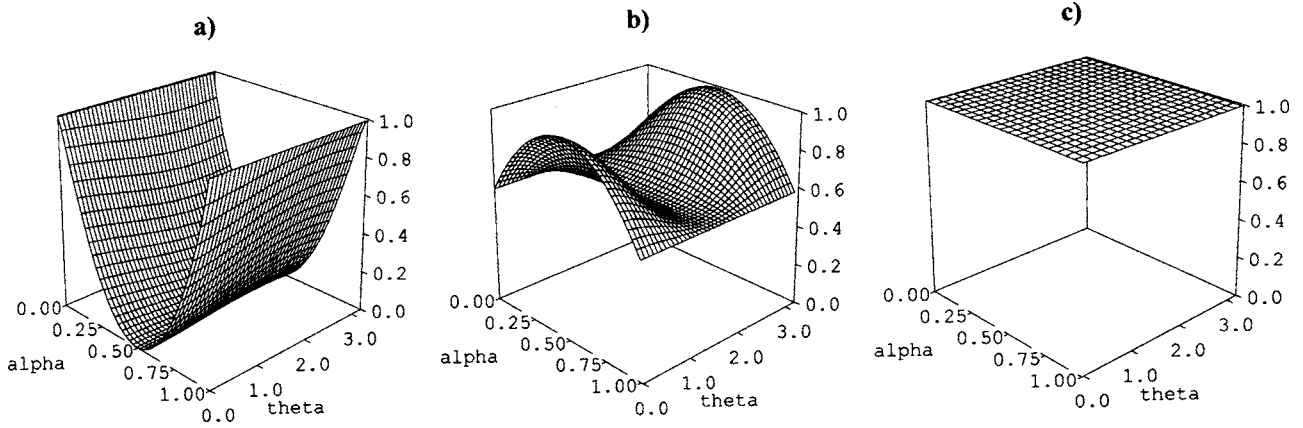


FIG. 1. Accuracy of the gate NOT as a function of the initial qubit state for the pulses optimized for (a) transitions (4) and (5), (b) transitions (11) and (12), and (c) transitions (4), (5), and (11).

phase difference  $\Delta\varphi \neq 0$  will lead to decrease in the transfer probability.

In order to explore this effect we have carried out a series of numerical experiments. First, we have numerically optimized the pulse shape using the functional (3) with two transitions, either (4) and (5) or (11) and (12). Then we have applied the optimal pulse to various initial qubit states generated by changing  $\alpha$  and  $\theta$  in expression (7). Finally, for each studied case we have computed the transfer probability  $P = |\langle \psi_f(T) | \phi_f \rangle|^2$ . Figure 1 shows  $P$  as a function of two variables,  $\alpha$  and  $\theta$ ; the  $P(\alpha, \theta)$  of the pulse represents the gate accuracy as a function of the initial qubit state. The results obtained with the pulse optimized for transitions (4) and (5) are presented in Fig. 1(a). Figure 1(b) gives the same for the pulse optimized for transitions (11) and (12). The readers can see that in both cases the gate accuracy is very high in the vicinity of the points used in the pulse optimization procedure: in Fig. 1(a) the value of  $P$  is nearly 0.995 at the points  $\alpha=0$  and  $\alpha=1$ ; in Fig. 1(b) it is about 0.995 at the points  $(\alpha=\frac{1}{2}, \theta=0)$  and  $(\alpha=\frac{1}{2}, \theta=\pi)$ . These numbers reflect precision of the OCT pulse optimization. However, in both examples the accuracy drops significantly when the values of  $\alpha$  and  $\theta$  are changed: in Fig. 1(b) near the  $\theta=\pi/2$  line it is only  $\sim 0.6$  and in Fig. 1(a) near the  $\alpha=1/2$  line we almost have  $P \sim 0$ .

Such a behavior of the numerical results correlates closely with the analytical results (10) and (14). Analysis of the derivative  $dP/d\alpha$  calculated from Eq. (10) allowed us to identify only one minimum of  $P(\alpha)$  at  $\alpha=\frac{1}{2}$ , which is consistent with Fig. 1(a). Note that the line  $\alpha=\frac{1}{2}$  represents the equator of the Bloch sphere<sup>16,17</sup> while the points  $\alpha=0$  and  $\alpha=1$  represent poles of the Bloch sphere; the surface of the Bloch sphere is mapped onto our  $(\alpha, \theta)$  plane. Similarly, analysis of the  $\partial P/\partial\alpha$  and  $\partial P/\partial\theta$  for Eq. (14) showed two local maxima at  $(\alpha=\frac{1}{2}, \theta=0)$  and  $(\alpha=\frac{1}{2}, \theta=\pi)$ , and a saddle point at  $(\alpha=1/2, \theta=\pi/2)$  consistent with Fig. 1(b).

Therefore, we conclude that neither of the two pulses analyzed in Figs. 1(a) and 1(b) represents a truly universal quantum gate. If the values of  $\alpha$  and  $\theta$  deviate from the values used in the pulse optimization the gate accuracy significantly drops. From Eqs. (10) and (14) it follows that in order to maintain  $P=1$  we should have  $\Delta\varphi=0$  for two tran-

sitions used. Analytically this gives us constant  $P=1$ , independent of  $\alpha$  and  $\theta$  as it should be. But, as explained in the Introduction, the total phase of the final state is not controlled in the OCT algorithm, i.e., it is arbitrary and is generally different for two optimized transitions. A practical way to constrain phases is to include a third transition,<sup>7</sup> for example, transition (11) for simultaneous optimization with transitions (4) and (5). It is easy to show that expressions (4), (5), and (11) can be satisfied simultaneously only if  $\varphi_1=\varphi_2=\varphi_3$ . To explore this possibility we have repeated the numerical experiment described above, now using the pulse optimized for three transitions simultaneously: (4), (5), and (11). Figure 1(c) represents the result of applying this pulse to an arbitrary initial qubit state. One can clearly see that the problem is now removed and the gate is accurate everywhere in the  $(\alpha, \theta)$  space, i.e., for any initial qubit state.

In Table I we summarized the results of this study: The gate accuracy  $P^k$  for each transition  $k$  involved in the optimization procedure is always high due to OCT. The phase difference  $\Delta\varphi$  between the two optimized transitions is large after the standard optimization, but is guaranteed to be small after the phase-constrained optimization. In the last column we give the gate *fidelity* calculated according to Ref. 4 as

TABLE I. Summary of optimization results for the gate NOT.

Transitions optimized	$P$	$\Delta\varphi$ (deg)	$F$
$ 0\rangle \rightarrow  1\rangle e^{i\varphi_1}$	0.995	175.9	0.001
$ 1\rangle \rightarrow  0\rangle e^{i\varphi_2}$	0.995		
$\frac{1}{\sqrt{2}}( 0\rangle+ 1\rangle) \rightarrow \frac{1}{\sqrt{2}}( 1\rangle+ 0\rangle) e^{i\varphi_3}$	0.995	79.2	0.591
$\frac{1}{\sqrt{2}}( 0\rangle- 1\rangle) \rightarrow \frac{1}{\sqrt{2}}( 1\rangle- 0\rangle) e^{i\varphi_4}$	0.995		
$ 0\rangle \rightarrow  1\rangle e^{i\varphi_1}$	0.996	0.2	0.997
$ 1\rangle \rightarrow  0\rangle e^{i\varphi_2}$	0.999		
$\frac{1}{\sqrt{2}}( 0\rangle+ 1\rangle) \rightarrow \frac{1}{\sqrt{2}}( 1\rangle+ 0\rangle) e^{i\varphi_3}$	0.999		
$ 0\rangle \rightarrow  1\rangle e^{i\varphi_1}$	0.997	0.7	0.997
$ 1\rangle \rightarrow  0\rangle e^{i\varphi_2}$	0.997		
$\frac{1}{\sqrt{2}}( 0\rangle+ 1\rangle) \rightarrow \frac{1}{\sqrt{2}}( 1\rangle+ 0\rangle) e^{i\varphi_3}$	0.999		
$\frac{1}{\sqrt{2}}( 0\rangle- 1\rangle) \rightarrow \frac{1}{\sqrt{2}}( 1\rangle- 0\rangle) e^{i\varphi_4}$	0.999		

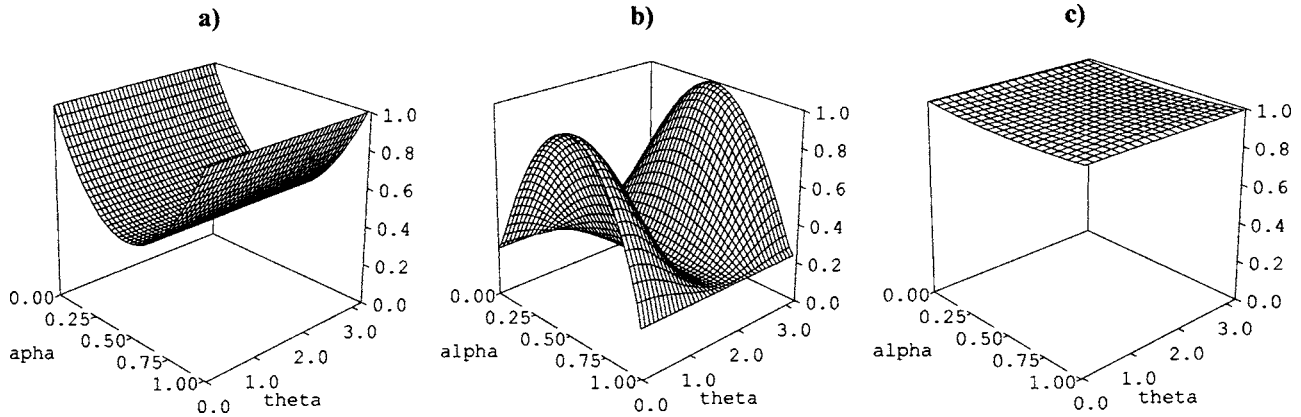


FIG. 2. Accuracy of the  $\pi$  gate as a function of the initial qubit state for the pulses optimized for (a) transitions (17) and (18), (b) transitions (19) and (20), and (c) transitions (17), (19), and (20).

$$F = \frac{1}{N^2} \left| \sum_{k=1}^N \langle \phi_j^k | \psi_i^k(T) \rangle \right|^2. \quad (15)$$

Here the sum is over two or more transitions optimized simultaneously. The fidelity is high only after the phase-constrained optimization when the phases of all the optimized  $\psi_i^k(T)$  are almost equal. Table I also demonstrates that optimizing all four transitions simultaneously: (4), (5), (11), and (12), gives only a minor numerical advantage since including three transitions is already enough to constrain the common phase.

### B. $\pi$ -rotation gate

The  $\pi$  gate, often represented as

$$\Pi|0\rangle \rightarrow |0\rangle,$$

$$\Pi|1\rangle \rightarrow -|1\rangle,$$

increases the phase difference between the qubit states  $|0\rangle$  and  $|1\rangle$  by  $180^\circ$ . Transformation of an arbitrary initial qubit state (7) by the  $\pi$  gate is therefore given by

$$\Pi(\sqrt{\alpha}|0\rangle + \sqrt{1-\alpha}e^{i\theta}|1\rangle) \rightarrow \sqrt{\alpha}|1\rangle - \sqrt{1-\alpha}e^{i\theta}|0\rangle. \quad (16)$$

The two-transition pulse can be optimized using the qubit eigenstates:

$$|0\rangle \rightarrow |0\rangle e^{i\varphi_1}, \quad (17)$$

$$|1\rangle \rightarrow -|1\rangle e^{i\varphi_2}, \quad \varphi_2 \neq \varphi_1. \quad (18)$$

Again, the  $\varphi_2 \neq \varphi_1$  reflects the fact that phases of the final states are not controlled in the OCT algorithm. Alternatively, using the superposition initial states, the two-transition pulse for the  $\pi$  gate can be optimized as

$$\frac{1}{\sqrt{2}}(|0\rangle + |1\rangle) \rightarrow \frac{1}{\sqrt{2}}(|0\rangle - |1\rangle) e^{i\varphi_3}, \quad (19)$$

$$\frac{1}{\sqrt{2}}(|0\rangle - |1\rangle) \rightarrow \frac{1}{\sqrt{2}}(|0\rangle + |1\rangle) e^{i\varphi_4}, \quad \varphi_4 \neq \varphi_3. \quad (20)$$

Repeating the derivations described in the previous section one can obtain from transitions (17) and (18) an equation for the transfer probability  $P(\alpha)$ ; this equation appears to be equivalent to formula (10). The expression for  $P(\alpha, \theta)$  ob-

tained from transitions (19) and (20) appears to be equivalent to formula (14) as well.

Numerical results obtained for the  $\pi$  gate are presented in Fig. 2 and are summarized in Table II. Again, the  $P(\alpha, \theta)$  of the pulse optimized for transitions (17) and (18) exhibits the minimum at the equator [see Fig. 2(a)] while the  $P(\alpha, \theta)$  of the pulse optimized for (19) and (20) shows two maxima and a saddle point [see Fig. 2(b)]. The general shapes of these surfaces are qualitatively similar to those shown in Figs. 1(a) and 1(b) for the gate NOT. Some quantitative differences between the data shown in Figs. 1 and 2 are also present. These differences are due to the different values of unconstrained  $\Delta\varphi \neq 0$  obtained in each case. For example, the NOT pulse optimized for transitions (4) and (5) shows  $\Delta\varphi \approx 180^\circ$  (see Table I) and from Eq. (10) we obtain  $P(\alpha) \sim 0$  at the equator, consistent with Fig. 1(a). In the case of the  $\pi$  gate the pulse optimized for transitions (17) and (18) shows smaller  $\Delta\varphi \approx 90^\circ$  (see Table II) and from Eq. (10) we obtain larger  $P(\alpha) \approx 0.5$  at the equator, consistent with Fig. 2(a).

In Fig. 2(c) we see again that optimizing three transitions simultaneously allowed us to fix the phase problem and obtain the pulse which provides the transfer probability close to

TABLE II. Summary of optimization results for the  $\pi$  gate.

Transitions optimized	$P$	$\Delta\varphi$ (deg)	$F$
$ 0\rangle \rightarrow  0\rangle e^{i\varphi_1}$	0.999	92.3	0.480
$ 1\rangle \rightarrow - 1\rangle e^{i\varphi_2}$	0.999		
$\frac{1}{\sqrt{2}}( 0\rangle +  1\rangle) \rightarrow \frac{1}{\sqrt{2}}( 0\rangle -  1\rangle) e^{i\varphi_3}$	0.994	120.8	0.242
$\frac{1}{\sqrt{2}}( 0\rangle -  1\rangle) \rightarrow \frac{1}{\sqrt{2}}( 0\rangle +  1\rangle) e^{i\varphi_4}$	0.994		
$ 0\rangle \rightarrow  0\rangle e^{i\varphi_1}$	0.995	0.3	0.976
$\frac{1}{\sqrt{2}}( 0\rangle +  1\rangle) \rightarrow \frac{1}{\sqrt{2}}( 0\rangle -  1\rangle) e^{i\varphi_3}$	0.973		
$\frac{1}{\sqrt{2}}( 0\rangle -  1\rangle) \rightarrow \frac{1}{\sqrt{2}}( 0\rangle +  1\rangle) e^{i\varphi_4}$	0.973		
$ 0\rangle \rightarrow  0\rangle e^{i\varphi_1}$	0.997	0.6	0.975
$ 1\rangle \rightarrow - 1\rangle e^{i\varphi_2}$	0.997		
$\frac{1}{\sqrt{2}}( 0\rangle +  1\rangle) \rightarrow \frac{1}{\sqrt{2}}( 0\rangle -  1\rangle) e^{i\varphi_3}$	0.975		
$\frac{1}{\sqrt{2}}( 0\rangle -  1\rangle) \rightarrow \frac{1}{\sqrt{2}}( 0\rangle +  1\rangle) e^{i\varphi_4}$	0.975		

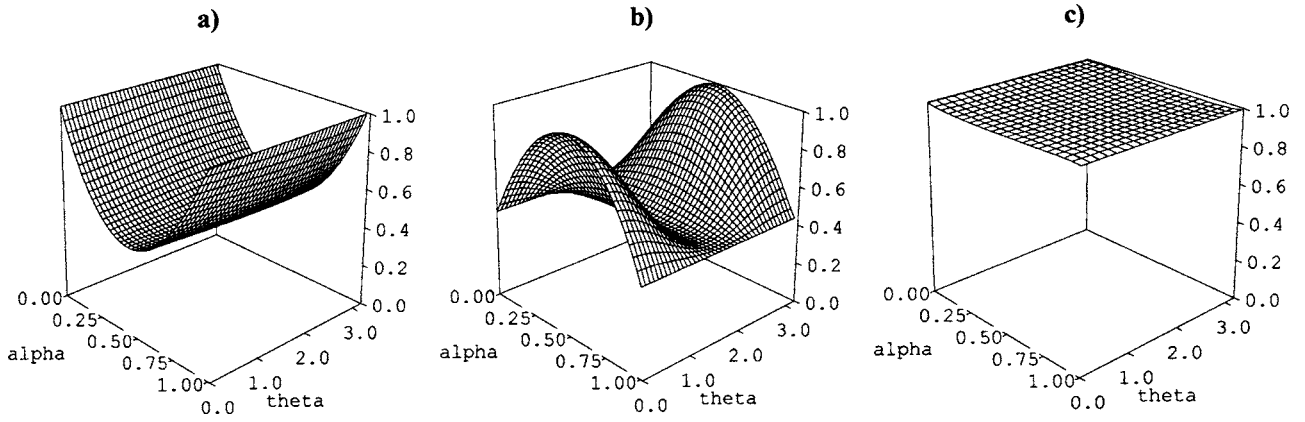


FIG. 3. Accuracy of the Hadamard transform as a function of the initial qubit state for the pulses optimized for (a) transitions (22) and (23), (b) transitions (24) and (25), and (c) transitions (22), (23), and (25).

$P=1$  everywhere in the  $(\alpha, \theta)$  space. Note that the phase difference  $\Delta\varphi$  is very small after such a phase-constrained optimization and the gate fidelity is high (see Table II).

### C. Hadamard transform

The Hadamard gate creates the equal probability superposition states out of the qubit eigenstates:

$$\text{Had}|0\rangle \rightarrow \frac{1}{\sqrt{2}}(|0\rangle + |1\rangle),$$

$$\text{Had}|1\rangle \rightarrow \frac{1}{\sqrt{2}}(|0\rangle - |1\rangle).$$

This transform, when applied to a qubit in an arbitrary initial state (7), should give us

$$\begin{aligned} \text{Had}(\sqrt{\alpha}|0\rangle + \sqrt{1-\alpha}e^{i\theta}|1\rangle) &\rightarrow \frac{1}{\sqrt{2}}(\sqrt{\alpha} + \sqrt{1-\alpha}e^{i\theta})|0\rangle \\ &+ \frac{1}{\sqrt{2}}(\sqrt{\alpha} - \sqrt{1-\alpha}e^{i\theta})|1\rangle. \end{aligned} \quad (21)$$

As for the other gates discussed above, the two-transition optimization can be based either on the pure initial eigenstates:

$$|0\rangle \rightarrow \frac{1}{\sqrt{2}}(|0\rangle + |1\rangle)e^{i\varphi_1}, \quad (22)$$

$$|1\rangle \rightarrow \frac{1}{\sqrt{2}}(|0\rangle - |1\rangle)e^{i\varphi_2}, \quad \varphi_2 \neq \varphi_1, \quad (23)$$

or, on the superposition initial states:

$$\frac{1}{\sqrt{2}}(|0\rangle + |1\rangle) \rightarrow |0\rangle e^{i\varphi_3} \quad (24)$$

$$\frac{1}{\sqrt{2}}(|0\rangle - |1\rangle) \rightarrow |1\rangle e^{i\varphi_4}, \quad \varphi_4 \neq \varphi_3. \quad (25)$$

When the pulse optimized for transitions (22) and (23), or alternatively (24) and (25), is analytically “applied” to a qubit in an arbitrary initial state (7) and the transfer probabilities  $P(\alpha)$  and  $P(\alpha, \theta)$  are computed for the Hadamard gate as we did it for the gate NOT, it appears that the expressions for  $P(\alpha)$  and  $P(\alpha, \theta)$  are again equivalent to formulas (10) and (14), respectively. Since Eqs. (10) and (14) are valid for all three major gates we suggest that these expressions are general. The rigorous proof of this postulate will be explored in the future.

The results of the OCT pulse optimizations for the Hadamard transform are given in Fig. 3 and Table III. They are qualitatively similar to the results obtained for the gates NOT and  $\pi$  rotation. Here we observed, again, that the pulses optimized for two transitions with arbitrary phases [either (22) and (23) or (24) and (25)] do not perform the desired transformation if the initial qubit state is changed [Figs. 3(a) and 3(b)]. However, the phase-constrained optimization with three transitions included: (22), (23), and (25), gives us a pulse characterized by a practically flat  $P(\alpha, \theta)$  shown in Fig. 3(c). Such a pulse performs accurate Hadamard transform on any initial state of the qubit. Also, Table III shows that optimization of four transitions simultaneously gives a little more accurate pulse.

For the three gates studied here the phase difference  $\Delta\varphi$  is dramatically reduced in the phase-constrained optimization compared to the unconstrained one. However, in the case of the Hadamard gate the residual  $\Delta\varphi \approx 10^\circ$  is still observed in the numerical results. Analysis has shown that the reason for not obtaining the perfect  $\Delta\varphi=0$  is related to the fact that the probability transfer is also not perfect (though it is very high). Indeed, in order to derive the equality  $\varphi_3=\varphi_2=\varphi_1$  from Eqs. (4)–(6) we had to assume that a complete

TABLE III. Summary of optimization results for the Hadamard gate.

Transitions optimized	$P$	$\Delta\varphi$ (deg)	$F$
$ 0\rangle \rightarrow \frac{1}{\sqrt{2}}( 0\rangle +  1\rangle)e^{i\varphi_1}$	0.999	96.1	0.446
$ 1\rangle \rightarrow \frac{1}{\sqrt{2}}( 0\rangle -  1\rangle)e^{i\varphi_2}$	0.999		
$\frac{1}{\sqrt{2}}( 0\rangle +  1\rangle) \rightarrow  0\rangle e^{i\varphi_3}$	0.999	95.7	0.448
$\frac{1}{\sqrt{2}}( 0\rangle -  1\rangle) \rightarrow  1\rangle e^{i\varphi_4}$	0.999		
$ 0\rangle \rightarrow \frac{1}{\sqrt{2}}( 0\rangle +  1\rangle)e^{i\varphi_1}$	0.996	13.8	0.982
$ 1\rangle \rightarrow \frac{1}{\sqrt{2}}( 0\rangle -  1\rangle)e^{i\varphi_2}$	0.996		
$\frac{1}{\sqrt{2}}( 0\rangle -  1\rangle) \rightarrow  1\rangle e^{i\varphi_4}$	0.985		
$ 0\rangle \rightarrow \frac{1}{\sqrt{2}}( 0\rangle +  1\rangle)e^{i\varphi_1}$	0.995	6.3	0.992
$ 1\rangle \rightarrow \frac{1}{\sqrt{2}}( 0\rangle -  1\rangle)e^{i\varphi_2}$	0.995		
$\frac{1}{\sqrt{2}}( 0\rangle +  1\rangle) \rightarrow  0\rangle e^{i\varphi_3}$	0.996		
$\frac{1}{\sqrt{2}}( 0\rangle -  1\rangle) \rightarrow  1\rangle e^{i\varphi_4}$	0.996		

transfer of probability is achieved by the laser pulse. In practice, however, small deviations in the probability transfer lead to some residual phase differences as well. This should cause no problem for the molecules that can be efficiently controlled.<sup>6</sup>

### III. CONCLUSIONS

We carried out very detailed OCT studies of the gates NOT,  $\pi$  rotation, and the Hadamard transform in the vibrational qubit with the focus on understanding how the phases of the optimized transitions affect the gate accuracy. We demonstrated that when the laser pulse is optimized for only two transitions in the qubit, the gate accuracy should be viewed as a function of three variables:  $\alpha$  and  $\theta$ , which define the initial qubit state, and  $\Delta\varphi$ , which represents the phase difference imposed by the pulse. We showed that if the  $\Delta\varphi$  is large (unconstrained) then the high quality of the pulse optimization achieved with the OCT algorithm is meaningful only in the close vicinities of the two initial qubit states used in the pulse optimization procedure. For other initial qubit states the gate accuracy can be significantly lower which means that such a laser pulse does not represent a truly universal quantum gate. We also confirmed the result of Ref. 7. Namely, we observed that simultaneous optimization of three transitions in the qubit allowed to constrain phases (provided the transition probabilities are high). We found that such a phase-constrained optimization produces laser pulses characterized by a small  $\Delta\varphi$ , consistently high accuracy, and a weak dependence on the initial qubit state. One of the possible future research directions is to search for alternative

direct ways of incorporating the efficient phase control into the OCT pulse optimization procedure.

### ACKNOWLEDGMENTS

This research was partially supported by NSF Grant No. PHY-045953. It also used resources of the National Energy Research Scientific Computing Center, supported by the Office of Science of the U.S. Department of Energy under Contract No. DE-AC03-76SF00098.

- <sup>1</sup>C. M. Tesch, L. Kurtz, and R. de Vivie-Riedle, Chem. Phys. Lett. **343**, 633 (2001).
- <sup>2</sup>C. M. Tesch and R. de Vivie-Riedle, Phys. Rev. Lett. **89**, 157901 (2002).
- <sup>3</sup>J. P. Palao and R. Kosloff, Phys. Rev. Lett. **89**, 188301 (2002).
- <sup>4</sup>J. P. Palao and R. Kosloff, Phys. Rev. A **68**, 062308 (2003).
- <sup>5</sup>U. Troppmann, C. M. Tesch, and R. de Vivie-Riedle, Chem. Phys. Lett. **378**, 273 (2003).
- <sup>6</sup>D. Babikov, J. Chem. Phys. **121**, 7577 (2004).
- <sup>7</sup>C. M. Tesch and R. de Vivie-Riedle, J. Chem. Phys. **121**, 12158 (2004).
- <sup>8</sup>U. Troppmann and R. de Vivie-Riedle, J. Chem. Phys. **122**, 154105 (2005).
- <sup>9</sup>Y. Ohtsuki, Chem. Phys. Lett. **404**, 126 (2005).
- <sup>10</sup>S. Suzuki, K. Mishima, and K. Yamashita, Chem. Phys. Lett. **410**, 358 (2005).
- <sup>11</sup>T. Cheng and A. Brown, J. Chem. Phys. **124**, 34111 (2006).
- <sup>12</sup>W. Zhu, J. Botina, and H. Rabitz, J. Chem. Phys. **108**, 1953 (1998).
- <sup>13</sup>K. Sundermann and R. de Vivie-Riedle, J. Chem. Phys. **110**, 1896 (1999).
- <sup>14</sup>E. Sundermann, H. Rabitz, and R. de Vivie-Riedle, Phys. Rev. A **62**, 013409 (2000).
- <sup>15</sup>G. K. Paramonov, Chem. Phys. **177**, 169 (1993).
- <sup>16</sup>G. Johnson, *A Shortcut Through Time: The Path to the Quantum Computer* (Knopf, New York, 2003).
- <sup>17</sup>N. G. Cooper and J. A. Schecker, *Information, Science, and Technology in a Quantum World* (Los Alamos National Laboratory, Los Alamos, NM, 2003).